2021-11-21

On the Scalability of Wave Energy Converters

Jin, S

10.1016/j.oceaneng.2021.110212
Ocean Engineering
Elsevier

On the Scalability of Wave Energy Converters

Siya Jin*, Siming Zheng, Deborah Greaves
School of Engineering, Computing and Mathematics, Faculty of Science and Engineering, University of Plymouth, PL4 8AA, UK

Abstract

To achieve cost parity with other renewables, the wave energy sector requires significant cost reduction. Increasing the wind turbine scale is one successful route to cost reduction in the wind industry. This paper aims at investigating the scalability of wave energy converters (WECs) and providing a thorough review and analysis of published data. Unlike wind turbines for which the energy absorbed increases with turbine diameter, the scalability of WECs is complicated and varies by WEC type. Here, we demonstrate that the point absorber (PA) WEC lacks scalability and has limited theoretical capture width (*CW*), although its theoretical capture width ratio (*CWR*) can exceed 100%. The *CW* increases with device width for terminator and length for attenuator WECs, demonstrating scalability, but *CWR* limits of 50% and 100% exist. Analysis of the practical performance data carried out in this work shows that: (1) due to the lack of scalability, it will be difficult for the PA unit to reach MW scale, and in most examples, the characteristic dimension is generally < 35 m; (2) the terminator could achieve MW scale by using a high characteristic dimension > 100 m; (3) the PA appears to work more efficiently than the terminator and attenuator (e.g., for the PA oscillating wave surge converters, hydrodynamic efficiencies up to 80% have been achieved in laboratory tests).

Keywords: Wave energy converter; Scalability; Theoretical and practical performance; Capture width; Capture width ratio.

* Corresponding author.
Email address: siya_jin@126.com (Siya Jin); siming.zheng@plymouth.ac.uk (Siming Zheng); deborah.greaves@plymouth.ac.uk (Deborah Greaves)

Nomenclature	
CW	Capture width
CWR	Capture width ratio
CfD	Contract for difference
DoF	Degree of freedom
LCoE	Levelised cost of energy
ORE	Offshore renewable energy
OWC	Oscillating water column
OWSC	Oscillating wave surge converter
PA	Point absorber
PTO	Power take-off
WEC	Wave energy converter
2D	Two-dimensional
3D	Three-dimensional

1. Introduction

Due to the growing concern over climate change, the use of renewable energies, such as wind, solar, wave and tidal for electricity generation is being actively explored throughout the world. Among these renewable energies, wind and solar energy have reached commercialisation; offshore wind is growing rapidly, and floating offshore wind is under innovation. Wave and tidal energy are at earlier stages of commercialisation; tidal energy is under demonstration and on the verge of becoming commercially viable (MeyGen, 2021) whereas wave energy development is currently at the research stage with a limited but growing number of demonstration projects around the world (OES, 2010–2020). Devices used to capture and convert wave energy into useful energy are known as wave energy converters (WECs). Wave energy has been a very active area of research since the 1970s in response to the oil crisis (UK-Parliament, 2001) and many studies have been carried out to evaluate and demonstrate the advantages and feasibility of different WEC technologies. For detailed information, see the series of reviews in the literature that cover performance and efficiency of WECs (Babarit, 2015; Aderinto and Li, 2019; Sheng, 2019), survivability and reliability (Coe and Neary, 2014; Coe et al., 2018), lessons learnt from the past and pathway to the reduction of levelised cost of energy (LCoE) of WECs (Bedard and Hagerman, 2004; ECORYS and Fraunhofer, 2017; Hannon et al., 2017; Smart and Noonan, 2018).

It is interesting to reflect on the development and growth of the wind and offshore wind sectors and to consider whether a similar path of development and cost reduction is achievable for wave energy. Reviewing the development of wind energy onshore and offshore, one key parameter that contributes to

the rapid advancement of this sector and has led to significant opportunities for cost reduction is the growth in size of wind turbines (Caduff et al., 2012; IRENA, 2019). As demonstrated in Fig. 1, the size of wind turbines has increased dramatically in the past 20 years, leading to increased levels of power generated from a single device and thus reducing the LCoE of wind power. As reported by the UK Government in 2020, the clearing price for offshore wind has dropped down to approximately £40/MWh, which is economically competitive with fossil-fuel alternatives to some extent (BEIS, 2020). For comparison, the cost of wave energy is still relatively high, with a strike price of £281/£268 MWh (for year 2023/2024 and 2024/2025) in the round 3 contract for difference (CfD) announced by the UK Government in 2019 (BEIS, 2019). In the newly released round 4 CfD, the relatively mature offshore wind has been put in a pot on its own, with wave, tidal and floating offshore wind allocated a separate pot for less established technologies. This approach aims to increase the bespoke support for marine energy and its contribution to the long-term decarbonisation of the UK energy system (BEIS, 2020).

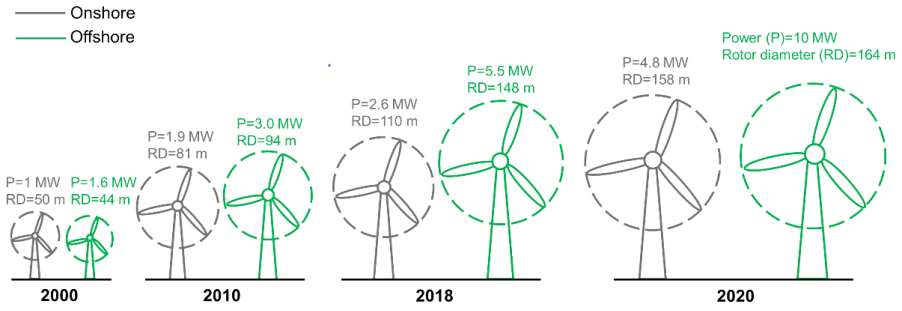

Fig. 1. The evolution of the onshore and offshore wind turbine size 2000–2020. The data is adapted from that given in IRENA (2019).

Compared with the converged and dominant design of three-bladed horizontal-axis turbines in the wind energy sector, there exist large variations in designs and concepts for WECs. WECs are generally classified by location and working principle as well as orientation & size (Antonio, 2010; AQUARET, 2012); there are many different technology concepts under development and no design convergence as yet. Following consultation through the scoping workshop held by the Supergen Offshore Renewable Energy (ORE) Hub in January 2020 and a series of structured interviews with industry professionals, a road map for wave energy development was produced (Greaves and Jin, 2020). The challenge of cost reduction for wave energy was considered, and whether, learning from the success of wind energy, wave energy can increase

the power generated and reduce the LCoE by increasing the device scale (Greaves et al., 2020). The aim of this paper is to address this question by quantifying the scalability of different WEC concepts in a thorough review and fresh analysis of published literature considering theoretical and practical approaches and datasets. The authors hope that the scalability of different WEC concepts summarised in this work can provide valuable guidance to device and project developers in the wave energy sector and useful information to researchers. In addition to the scalability, evaluating the potential cost reduction of wave energy from aspects of reliability, survivability, accessibility, operation, and maintenance should be carefully conducted. This evaluation is beyond the scope of this paper and, therefore, left for future work. The remainder of the paper is organised as follows: general information of WECs is described in Section 2; theoretical scalability of different WECs is analysed in Section 3; practical scalability performance of different WECs and recommendations for future WECs are summarised in Section 4; and finally, conclusions are given in Section 5.

2. General information

2.1. Classification of wave energy converters

The exploration of WEC technology dates back to 1799 when an oscillating water column (OWC) type of WEC was first applied for electricity generation (Falnes, 2007). Since then, more and more types of WEC have been developed for different applications, locations and metocean conditions (Aderinto and Li, 2018). Here a brief review of the classification of WECs is given to provide some context for this study. Categories of WEC are illustrated in terms of operating principle (see Fig. 2) and orientation & size with respect to the wave front (see Fig. 3). Some novel concepts like the flexible membrane devices or hybrid devices are not considered in this study due to the limited available information (AWS; Yde et al., 2015; Babarit, 2017; Collinsa et al., 2021).

Based on operating principle (see Fig. 2), WECs can be classified as oscillating body, OWC and overtopping devices. An oscillating body type WEC converts wave motion into device oscillations to generate electricity. Some oscillating WECs are developed with multi-modes to absorb more energy. For simplification, three main sub-categories are further classified in this work based on the WEC's dominant oscillating mode: (1) heaving body, which is driven by wave action to oscillate in vertical motion; (2) oscillating wave surge converter (OWSC) that rotates around a hinged axis parallel to the wave crests; (3) articulated body that is oriented parallel to the wave direction and produces relative rotation between

adjacent segments. Examples of a heaving body WEC are Corpower (CORPOWER, 2021), LifeSaver (Even, 2019), Seabased (SEABASED, 2021), PowerBuoy® (OPT, 2021), CETO (Carnegie, 2021); examples of OWSC are Oyster (Henry et al., 2010), WaveRoller® (WaveRoller, 2021), bioWAVE™ (BioWave, 2015), CCell-Wave (CCell-Wave, 2021), Resolute Marine (Marine, 2021); examples of articulated body are Pelamis (Pelamis, 2004), SeaPower (SEAPOWER, 2021), Blue Star & Blue Horizon (Mocean, 2021), M4 WEC (Santo et al., 2020), Cockerell raft (Haren, 1979), MacCabe Wave Pump (Kraemer et al., 2001) and DEXA (Zanuttigh et al., 2013).

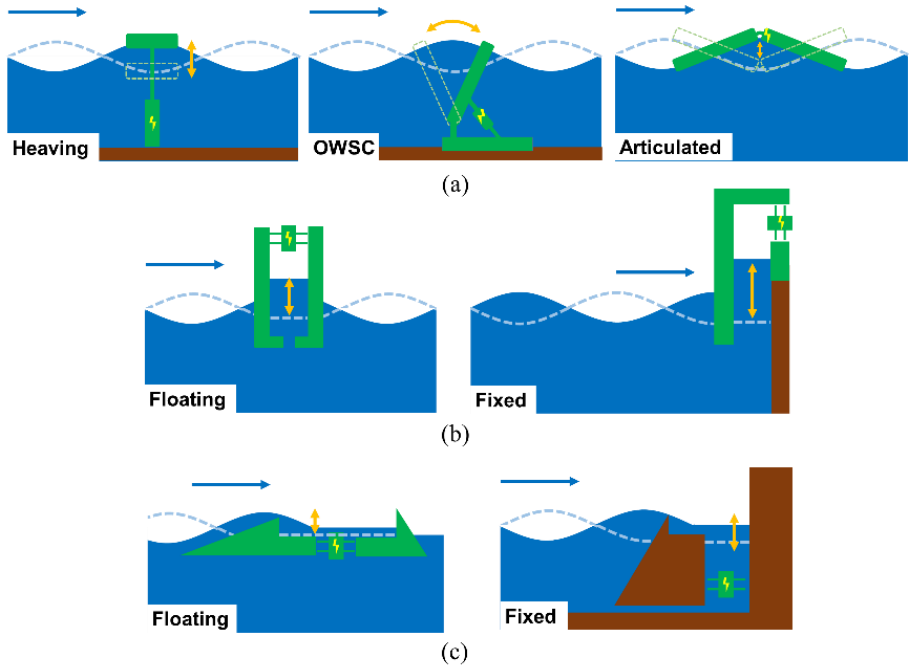

Fig. 2. Categories of WEC technologies classified by working principles. (a) Oscillating body including three popular applications: heaving body, oscillating wave surge converter (OWSC) and articulated body. (b) Oscillating water column (OWC) including floating and fixed type. (c) Overtopping including floating and fixed type.

The OWC uses trapped air above a water column to drive turbines for electricity generation. Fixed OWCs can be sited onshore or embedded into breakwaters, whereas floating OWCs can be installed offshore in deeper water. Examples of floating OWC are the OE buoy (OceanEnergy, 2020), Spar Buoy (Gomes et al., 2013), MARMOK-A-5 (MARMOK-A-5, 2016), Mighty Whale (Osawa et al., 2002), KNSWING (Nielsen and Thomsen, 2019), NEL OWC (Rendel and Tritton, 1982); examples of fixed OWC are Mutriku (Torre-Enciso et al., 2009), REWEC3 (Ghisu and Carabotta, 2017), Wavegen Limpet (Boake et al., 2002).

Overtopping devices cause waves to overtop into a reservoir to generate a head flow and subsequently drive turbines for electricity generation. Fixed devices can be sited onshore or integrated into breakwaters. Floating overtopping devices can be installed offshore. Examples of overtopping WECs are: floating Wave Dragon (WaveDragon, 2017) and fixed OBREC (Iuppa et al., 2019) and Tapchan (Mehlum, 1986).

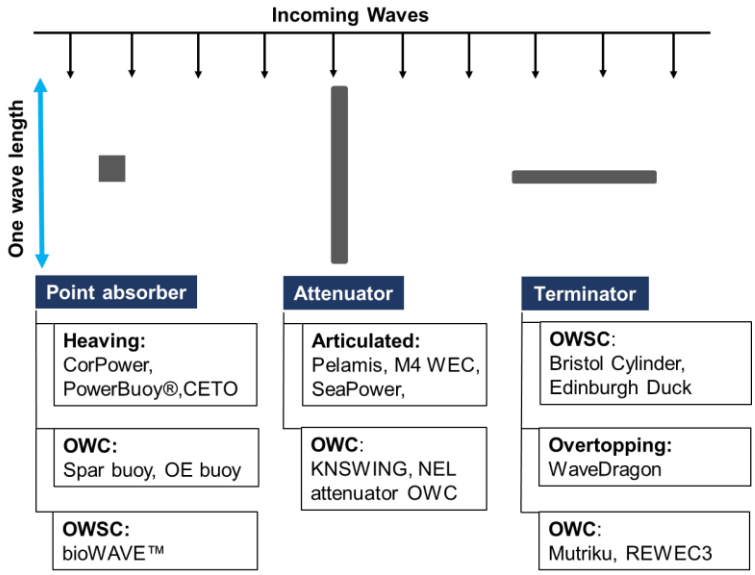

Fig. 3. Categories of WEC technology classified based on their orientation & size and the sub-categories with respect to working principle.

Based on size & orientation with respect to the wave front (see Fig. 3), WECs can be classified into three types: point absorber (PA), attenuator and terminator. For a PA, its dimension is much smaller than the incoming wave. For an attenuator, its length is comparable to or even larger than one wavelength and the device is oriented in parallel with the wave direction. The width of a terminator is comparable to or even larger than the incident wavelength and the device is aligned perpendicular to the wave direction. As can be seen from Fig. 3, the WEC categorizations based on orientation & size can be further divided into sub-categories according to the working principles. This diagram illustrates the complexity of WEC classification and terminology, which indicates the complexity of quantifying scalability of WECs, as discussed in Sections 3 and 4.

2.2. Quantifying performance

Two parameters are generally available for quantifying the power performance of a WEC and are used to assess the scalability characteristics of a WEC in this work. The first is the capture width (*CW*) in meter units, which is defined as the ratio of the power P_{wec} (unit of kW) extracted by a WEC to the wave energy flux *F* (unit of kW/m), where the wave energy flux represents the wave power available per metre of the wave crest width (as described in Fig. 4).

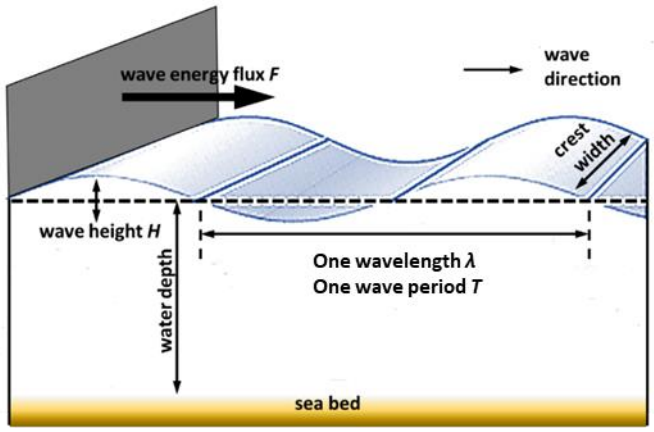

Fig. 4. Schematic descriptions of wave energy flux *F*, wave height *H*, wave period *T* and wavelength λ.

$$\boldsymbol{CW = \frac{P_{wec}}{F}} \quad \textbf{(1)}$$

In deep, realistic sea states, the energy flux may be approximated as $F \approx 0.5(\mathrm{kWm^{-3}s^{-1}}) * Hs^2Te$ (Beyene and Wilson, 2006; Cornejo-Bueno et al., 2016) where *Hs* is the significant wave height and *Te* is the wave energy period. Then,

$$\boldsymbol{P_{wec} \approx 0.5 Hs^2 Te * CW} \quad \textbf{(2)}$$

For a sinusoidal regular wave, $F \approx (\mathrm{kWm^{-3}s^{-1}}) * H^2T$ (Falnes and Kurniawan, 2020) where *H* is the wave height and *T* is the wave period. Then,

$$\boldsymbol{P_{wec} \approx H^2 T * CW} \quad \textbf{(3)}$$

The second parameter is the capture width ratio (*CWR*), which is the ratio of *CW* to the characteristic dimension *D* of a WEC. *CWR* is dimensionless and can be expressed as a percentage. It is similar to the

efficiency of a WEC and represents the ratio of the absorbed power by a WEC to the available wave power in a given width of wave crest.

$$\boldsymbol{CWR = \frac{CW}{D} = \frac{P_{wec}}{F * D}} \quad \textbf{(4)}$$

It should be noted that *CWR* can be over 100% as a result of the 'antenna effect' where the *CW* is larger than *D*, representing conditions in which the WEC can absorb more energy than contained in a wave crest of the same width. This phenomenon is explained in Section 3.

The characteristic dimension *D* of a WEC generally refers to the front width of the device orthogonal to the wave propagation direction. For example, for a cylindrical heaving WEC, the device diameter *A* is the characteristic dimension *D*; for an OWSC, the device width *W* is the characteristic dimension; nevertheless, for an attenuator type of articulated body, instead of using width, the device length *L* or the typical wave length λ is used as the characteristic dimension (Stansby et al., 2015). For more examples, see the information summarised in the database in the Appendix A.

3. Theoretical scalability of different wave energy converters

When considering scalability, we are concerned with whether the amount of power produced will increase with the increasing size of the individual device unit. For a wind turbine, there is a theoretical limit of 59.3% on the proportion of power absorbed by the turbine in a stream of fluid (Betz 1920). This is known as the 'Betz Limit' and is equivalent to an upper limit on the *CWR* (similar to the efficiency) of a WEC. It limits the percentage power capture of a given turbine diameter but does not limit the scalability of the wind turbine, because the power produced by the turbine is proportional to the turbine diameter squared. In other words, a wind turbine is not limited by a theoretical *CW* and a larger turbine generates higher power.

The theoretical maximum *CW* and *CWR* values have been well established for different types of WECs under the general assumptions that the wave is linear; the WEC motions are small; the power take-off (PTO) is simplified as a linear spring-damper system; the optimal control is achieved and the WEC motions are not constrained (Budal and Falnes, 1975; Evans, 1976; Mei, 1976; Newman, 1976; Henry et al., 2018; Falnes and Kurniawan, 2020). In this section, the theoretical *CW* and *CWR* values are comprehensively reviewed and analysed to assess theoretical scalability for different types of WEC.

3.1 Theoretical analysis with working principle

3.1.1 Heaving body

Budal and Falnes (1975) and Evans (1976) established the theoretical formula for the maximum *CW* of an axisymmetric rigid body oscillating in different degrees of freedom (DoF). This kind of device is generally regarded as a 3-dimensional (3D) case and named PA because its horizontal extent is much smaller than one wavelength (Journée and Massie, 2001) and it absorbs energy from all directions.

$$\boldsymbol{CW_{max} = \frac{N\lambda}{2\pi} \approx 0.16N\lambda,} \tag{5}$$

where CW_{max} is the theoretical maximum capture width; λ is the wavelength; N is related to the number of independent hydrodynamic DoF (Greaves and Iglesias, 2018). When the device oscillates in heave, $N = 1$, and $N = 2$ for either pitching or surging motion. It should be noted that surge and pitch motions are not independent of one another for an asymmetrical body. This means that if surge motion is already active and optimized, it is not possible to improve the *CW* by also exciting a pitch response. This has been validated by Newman (1976). Similarly, if a device is optimised for pitch, its *CW* cannot be improved by adding surge. In Newman's study, the maximum wave power absorbed by an axisymmetric rigid body, oscillating in surge, heave and pitch was derived. It was concluded that exciting two oscillating modes, either heave & pitch or heave & surge, is sufficient to achieve the maximum capture width of $3\lambda/2\pi \approx 0.48\lambda$ (i.e., $N = 3$), and thus a third mode was not needed. More recently, it was demonstrated that these rigid-body limits could be extended without bound (theoretically at least) by allowing an axisymmetric device to operate and absorb energy through the use of 'generalised (non-rigid body) modes' of motion (Porter et al., 2021). The present work is focused on the rigid body structured WECs, hence the 'generalised (non-rigid body) modes' associated work is not further discussed here.

Within linear wave assumptions and in offshore deep water, wavelength as a function of T is described as, $\lambda = gT^2/2\pi$ (g is the acceleration due to gravity). Then, Eq. (5) can be transformed as:

$$\boldsymbol{CW_{max} \approx \frac{NgT^2}{4\pi^2}} \tag{6}$$

Regarding Eqs. (3) – (6), we can find that the theoretical CW_{max} and the corresponding *CWR* show different sensitivity to the device's characteristic dimension, for an axisymmetric rigid oscillating body as presented in Fig. 5.

Unlike for the wind turbine, a WEC acting as a PA does not have an upper limit on *CWR*. As a result, the CW_{max} is not related to the PA's dimension (i.e., diameter) but highly dependent on the wave climate and the oscillating mode. There exists a specified CW_{max} at each wave condition for different oscillating modes. The CW_{max} shows a positive relationship with the wave period and wavelength. This supports the intuitive concept of deploying WECs in locations with energetic resources. In reality, it is more complex than that. With the evaluation of the effects from downtime, survivability, accessibility and cost for operation & maintenance, several studies have suggested that the moderate/milder resources may be more beneficial for WEC deployments compared to the energetic resources (Lavidas 2020, Lavidas and Blok 2021).

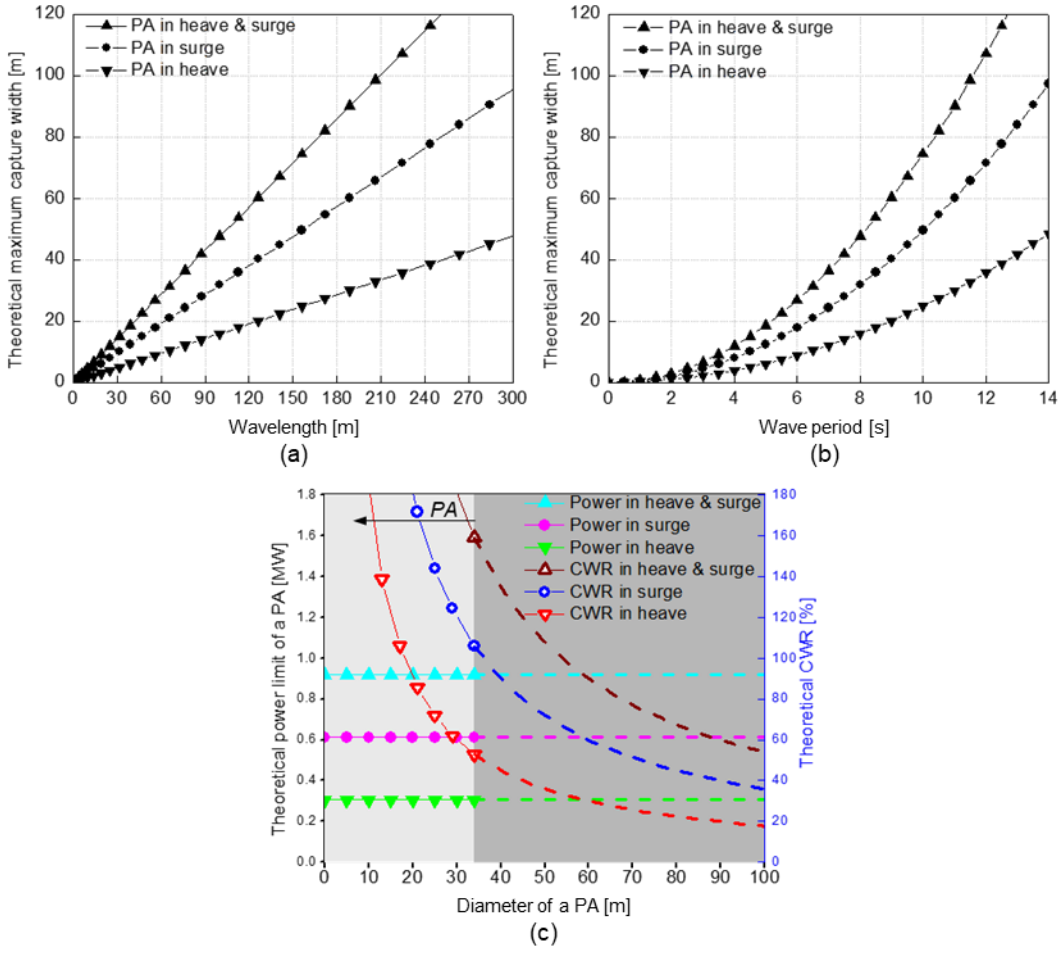

Fig. 5. Theoretical performance of an axisymmetric rigid body (PA) in heave, surge, and heave & surge. (a) The CW_{max} as a function of wavelength. (b) The CW_{max} as a function of wave period. (c) The theoretical maximum power extracted and related *CWR* at Hs = 2 m, Te = 8.5 s (i.e., $\lambda \approx 113$ m). The light grey background is used to clarify the PA defined as $A << \lambda$ (for reference, $A/\lambda = 0.3$, is used here). Values greater than the diameter of the PA are plotted in dashed lines without symbols.

Considering the marine energy test site of EMEC in the UK and selecting the annually most probable wave condition with Hs = 2 m and Te = 8.5 s (Santo et al., 2017), we can see that CW_{max} is limited by approximately 18 m, 36 m and 54 m for a PA in heave, surge and in heave & surge together, respectively. Then, as shown in Fig. 5(c), regardless of the PA's diameter, the corresponding theoretical maximum capacities are constant at approximately 0.3 MW, 0.6 MW and 0.9 MW for PAs in different oscillating modes (calculated from Eqs. (2) and (5)). As a result, with the same diameter, a PA oscillating in heave & surge has the highest efficiency, followed by that oscillating in surge and finally in heave. For PAs designed for a given mode of oscillation, the *CWR* appears to increase with the decrease of the device's diameter, as found by Evans (1976). More importantly, in theory, a heaving PA can be highly efficient with $CWR \geq$ 100% when the device diameter is ≤ 16% of one wavelength (as stated in Eq. (5) and Fig. 5). Hence, we can see that although without scalability, a PA with diameter $A \leq CW_{max}$ and multiple DoF response is recommended to achieve high performance efficiency. Note that the theoretical *CWR* mentioned here only considers the natural hydrodynamic conversion efficiency of the device in ideal fluid under linear assumptions and does not consider the mechanical efficiency of the PTO.

The phenomenon of *CWR* greater than 100% is known as the 'antenna effect', in which a PA can absorb energy from a wave front width greater than its physical dimension. This phenomenon was discovered by Budal and Falnes (1975) using a theoretical study based on a cylindrical heaving PA with diameter of 16 m, for which a *CW* of 25 m was obtained and as a result, *CWR* of 156.25% was achieved.

3.1.2 OWSC

Unlike an axisymmetric rigid oscillating body, for OWSC, both theoretical CW_{max} and corresponding *CWR* show clear sensitivity to the device's characteristic dimension. First, if the OWSC's width is relatively small compared with the incoming wavelength, the device will act approximately as a PA in surge motion (Henry et al., 2018), and corresponding hydrodynamic features will perform as that described in Section 3.1.1. As a result, the theoretical CW_{max} will be 0.32λ based on Eq. (5) and *CWR* greater than 100% can be achieved (see Fig. 5(c), *CWR* in surge). Therefore, regarding OWSC simply as a terminator, is not necessarily correct and an OWSC that is small relative to the wavelength operates more like a PA (Henry et al., 2010; Renzi and Dias, 2012; Henry et al., 2018).

If the OWSC's width is relatively long compared to the incident wavelength, the device will act approximately as a two-dimensional (2D) body with surge motion and can be regarded as a terminator. In

this case, the fundamental theory for a 2D oscillating device should be applied, which was established by Evans (1976) and clearly summarised by Falnes and Kurniawan (2020) as below:

$$\boldsymbol{CWR_{max} = \frac{1}{1 + |H_1/H_2|^2}} \quad \textbf{(7)}$$

H_1 is the complex amplitude of the wave generated by the device in the far field, in the direction of wave propagation; H_2 is the complex amplitude of the wave generated by the device in the far field, in the opposite direction of wave propagation. Based on Eq. (7), it is clear that for an OWSC with long width, there exists an upper limit on *CWR*, i.e., $CWR_{max,}$ which is similar to the Betz limit for a wind turbine.

Considering a symmetric body oscillating in surge or heave, equal waves are radiated in opposite directions with $|H_1| = |H_2|$ (Falnes and Kurniawan, 2020). Hence, the CWR_{max} of a symmetrical 2D OWSC oscillating in one single DoF is theoretically limited by 50%, whereas CWR_{max} can achieve 100% if the geometry of the OWSC is asymmetrical. In this case, the capture width, or power produced, will scale with the device dimension, and we can then expect that a wider OWSC can have a larger *CW* and a higher power capacity. This indicates that there exists scalability for a wide 2D OWSC, i.e., terminator, in theory.

3.1.3 Articulated body

Newman (1979) proposed the fundamental formula to achieve the CW_{max} of an articulated body as described in Eq. (8). The theory has been further discussed by Farley (1982), Rainey (2001), Stansell and Pizer (2013). It should be noted that the theory is based on the assumptions that the device's width-length ratio is small, typically 0.1 or 0.2 and each segment performs a small vertical movement varying slowly and continuously along the body's length.

$$\boldsymbol{CW_{max} = X(L, \lambda) * \lambda/2\pi,} \quad \textbf{(8)}$$

where $X(L, \lambda)$ the dimensionless capture width, is as a function of the device length L and wavelength λ, as presented in Fig. 6.

As shown in Fig. 6, it is important to note that there exists scalability for an articulated body, but it is not linearly related to the device length. The increase in the length of an articulated body does not produce a proportional increase of X. As a result, the increasing device length cannot contribute to a proportional increase in power extracted but may be at the expense of proportional structure cost. As can be seen, when

the device length is equal to one wavelength at $L = \lambda$, $X = 3.162$ can be achieved; when L is increased by 100% at $L = 2\lambda$, X is increased by only 45%, to 4.583. Hence, we can notice that articulated body WECs are generally designed with length comparable to one wavelength, such as the designs for M4 (Stansby et al., 2017), DEXA (Zanuttigh et al., 2013), and Mocean Energy (McNatt and Retzler, 2020).

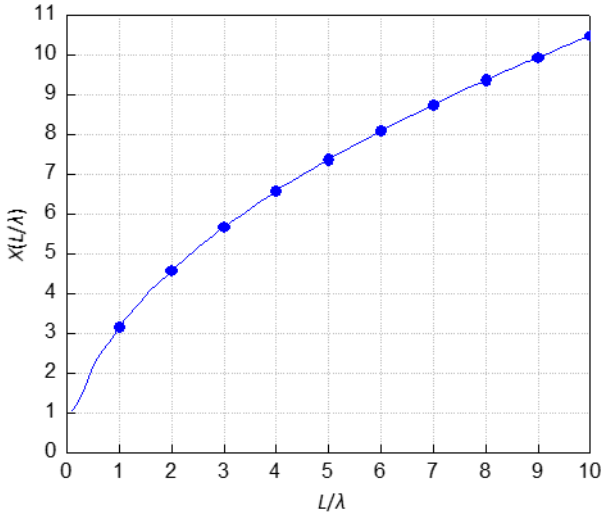

Fig. 6. Theoretical dimensionless capture width X (L, λ), from Eq. (8) (Stansell and Pizer, 2013) as a function of the ratio between the articulated body length L and wavelength λ.

3.1.4 OWC

Evans (1978) derived the fundamental theory for fixed OWCs based on the assumption that the internal free surface behaves as a weightless rigid piston with specified added mass and damping. In the work, theoretical values for both 2D and 3D cases were derived. Such a theory does not correctly model the hydrodynamics, because the boundary condition at the free surface inside the OWC chamber is not exactly satisfied. Despite this, it gives a good approximation for low frequencies, when the wavelength is very large compared to the horizontal length of internal water surface. As opposed to this rigid piston approximation, more accurate, pressure distribution models were proposed to study the performance of a 2D onshore and offshore OWC (Falnes and McIver, 1985; Evans and Porter, 1995; He et al., 2019). Analytical studies on the 3D offshore and onshore axisymmetric OWCs based on the pressure distribution models were carried out (Evans and Porter, 1997; Martins-Rivas and Mei, 2009; Zheng et al., 2019). The following findings were observed, for both the rigid-piston approximation and the pressure distribution models.

First, considering an offshore floating axisymmetric OWC with a single internal free surface, the device acts as a 3D case and the corresponding CW_{max} is identical to that of an axisymmetric rigid body oscillating

in heave, as described in Eq. (5). Additionally, it is theoretically possible for the device to capture energy from a wave front width greater than its characteristic dimension, resulting in *CWR* over 100%.

Second, the CWR_{max} of a 3D onshore axisymmetric OWC is affected by the incident wave direction, and it operates best under normal incidence at almost all frequencies (Martins-Rivas and Mei, 2009; Zheng et al., 2019). The CWR_{max} averaged over all incident wave directions is twice the CWR_{max} of an offshore axisymmetric OWC, which is the consequence of coastal reflection doubling the amplitude of the incident wave (Martins-Rivas and Mei, 2009).

Third, for a symmetric cubic OWC with relatively large width along the wave crest, acting as a 2D case, a CWR_{max} of 50% was obtained, which is identical with that described in Eq. (7) (Mavrakos and Konispoliatis, 2012). In addition, for a 2D asymmetrical OWC deployed offshore or onshore, the upper limit CWR_{max} of 100% can be achieved (Evans and Porter, 1995; He et al., 2019).

3.2 *Theoretical analysis with device orientation & size*

The study presented in Section 3.1 shows that the theoretical scalability of a WEC is more related to its orientation & size than its working principle. To investigate this further, we summarise the theoretical maximum performance of different WECs classified by device orientation & size in Table 1. Additionally, Fig. 7 provides a comparison of the theoretical maximum extracted power for different types of WEC at Hs = 2 m and Te = 8.5 s, from Eqs. (5) to (8), as a function of the characteristic dimension in device length, diameter, or width. As can be seen, unlike for wind turbines, the scalability of wave energy is more complex, and it varies with the type of the WEC classified by orientation & size.

Table 1. Theoretical scalability, CW_{max} and CWR_{max} of different WEC concepts classified by device orientation & size.

Orientation & size	**Theoretical scalability**	**Characteristic dimension [m]**	**Key characteristics**	**Working principles**	$\boldsymbol{CW_{max}}$ **[m]**	$\boldsymbol{CWR_{max}}$
PA	✗	Diameter (A)	Axisymmetric rigid 3D body with $A << \lambda$, Eq. (5)	1 DoF in heave	0.16λ	N/A
				1 DoF in surge	0.32λ	N/A
				Multi DoF, e.g., heave & surge or heave & pitch but not surge & pitch	0.48λ	N/A
Attenuator	✓	Length (L)	Slender body with device length $L \geqslant \lambda$. Eq. (8)	$L = \lambda$	0.51λ	N/A
				$L = 2\lambda$	$0.73\ \lambda$	N/A

Terminator	✓	Width (W)	2D device with $W \geqslant \lambda$, Eq. (7)	Symmetric with 1 DoF in heave or pitch or surge	$0.5W$	50%
				Symmetric with multi DoF, e.g., heave & pitch or heave & surge but not surge & pitch	W	100%
				Asymmetric	W	100%

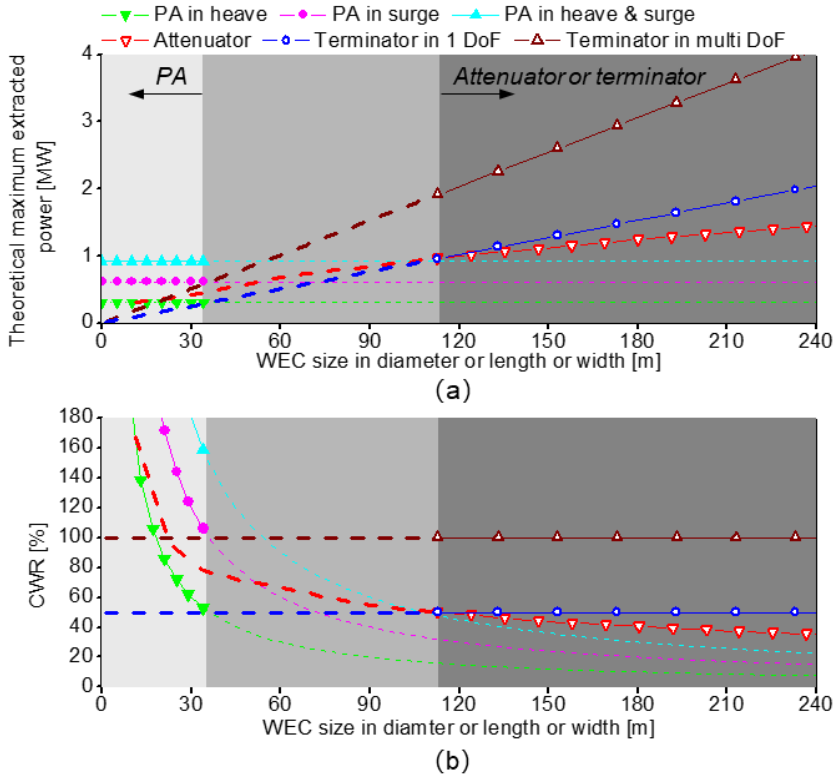

Fig. 7. Performance of different types of WECs at Hs = 2 m and Te = 8.5s (i.e., $\lambda \approx 113$ m). The graded grey background is to clarify the PA ($A << \lambda$), attenuator ($L \geqslant \lambda$) and terminator ($W \geqslant \lambda$). Values outside the size range of each type of WEC are plotted in dashed lines without symbols. (a) Theoretical maximum power extracted by each type of WEC as a function of the device size. (b) Corresponding *CWR* for each type of WEC as a function of the device size.

As summarized in Table 1 and presented in Fig. 7, a PA with diameter $A << \lambda$ is not scalable. The theoretical CW_{max} (i.e., the maximum extracted power) cannot be scaled by changing the PA's diameter but is limited by the oscillating modes and the wave climate. Regardless of the diameter, a PA which has more degrees of oscillating modes (hydrodynamically free) or is subject to longer waves (i.e., higher wave period), would achieve larger CW_{max}. Under a specified wave condition, a larger device would lead to a smaller *CWR* and a smaller device has a larger *CWR*. Therefore, a well-designed PA can be optimised to extract wave energy

from a greater width of wave front than its diameter, and this can achieve hydrodynamic efficiency greater than 100% (as presented in Fig. 7(b)). However, in this case, the response amplitude would be very large, so that the linear assumptions of small oscillations may be violated. Numbers of studies have evaluated the theoretical CW_{max} under motion constraints which are not further discussed here. For detailed information, see Evans (1981), Pizer (1993), Stansell and Pizer (2013), Wu et al. (2017), Cotten and Forehand (2020).

In contrast, an attenuator WEC that is in-line with the wave direction and with length $L \geqslant \lambda$, does exhibit scalability. However, it is important to note that the rate of increase in the maximum power extracted by an attenuator reduces with increasing length, because the theoretical *CW* does not increase linearly with the device length (see Table 1 and Fig. 7(a)). Similarly, scalability is also exhibited in theory by the terminator WEC, which is aligned perpendicular to the wave propagation and with width $W \geqslant \lambda$. With the theoretical *CWR* limit of 50% or 100%, the theoretical *CW* is proportional to the terminator width (see Fig. 7(a)).

In summary, the comparison of the performance for different WECs is presented in Fig. 7. Obviously, scalability works differently for each type of WEC. In addition, the scalability shows clear differences for the same type of WEC but with different oscillating modes activated to extract energy, such as the terminator, which has greater scaling properties when acting with multiple DoF than with single DoF. Therefore, it may not be a logical approach for wave energy to follow the successful steps of wind energy in aiming to reach technology convergence and cost reduction through scaling up a given device. Instead, we may need to take advantage of the variety of wave energy technologies and apply them rationally to specific applications and locations.

For example, as shown in Fig. 7(a), regardless of the size, a single PA cannot reach MW scale due to the *CW* limit, however, the very high *CWR* that may be achieved can be exploited in design. This highlights that for the development of PA, instead of adopting larger and larger devices to achieve MW scales, it may be more effective to develop kW scale devices, further explore the potential for high performance efficiency and focus on large array scale solutions. The PA may also be ideally suited for niche applications, such as desalination, mariculture and offshore oil & gas application, etc., to facilitate its commercialisation (Jin and Greaves, 2021). Benefitting from their scalability, terminator and attenuator WECs are capable of reaching MW scale by enlarging the device width or length, as presented in Fig. 7. However, it should be noted that the increase of attenuator length cannot yield increased power extraction in direct proportion, and so it is

important to carefully design the length of the attenuator, making a trade-off between the scalability and the construction cost.

4. Practical scalability of different wave energy converters

The summarised theoretical CW_{max} and CWR_{max} and their characteristics discussed in previous section are good indications of the behaviours of different types of WEC, but the linear hydrodynamics analysis contains simplifications and assumptions that may be violated in practice. Instead of being linear and monochromatic, the sea is non-linear, non-directional and polychromatic in practice. In addition, technical challenges from the motion constraints, mooring effects, PTO, wave forecasting and implementation of the 'optimal control', etc., remain to be overcome. Thus, the practical *CWR* is also a useful measure to present the performance of a WEC device and takes account of the practical effects from the PTO, mooring and non-linear waves, etc.

In this section the practical *CWR* is selected as a measure to further discuss the practical scalability of different WECs. Inspired by Babarit (2015), a newly updated database considering the information of 161 WEC cases is summarised and described in Appendix A. The database includes practical *CWR*s achieved from field, laboratory, and numerical tests. Although there exist uncertainties raised by the limited sample number, the variation of WEC specifications, tested wave resources, and variation in test conditions, we aim to use these accessible data to present an overall picture of the real-world performance of wave energy devices tested to date. More importantly, by comparing the practical performance to the theoretical scalability summarised in Section 3, recommendations for the development of future WEC are suggested here.

4.1 Analysis of the practical CWR

Using the database in Appendix A, practical *CWR*s are presented in Fig. 8 according to the WEC working principle and orientation & size as a function of the WEC's characteristic dimension. As can be seen, the WECs' characteristic dimensions and the practical *CWR*s vary significantly with working principle or orientation & size.

As observed from Fig. 8(b), overtopping devices have the maximum range of up to 300 m in characteristic dimension, followed by < 150 m for the OWC, 40–150 m for the articulated body, < 80 m for the OWSC and < 30 m for the heaving body. Combined with Fig. 8(c), the reason for the wide size range for overtopping, OWC and OWSC is that some of them belong to terminator and attenuator WEC types with

large characteristic dimension, while others belong to the PA type with small dimension. For comparison, all the practical heaving bodies are working as PAs with typical small dimension < 35 m. Therefore, it should be noted that the common misconception of regarding PA as a heaving body misses the point that OWSC, OWC and overtopping WECs with small characteristic dimensions all belong to the PA category.

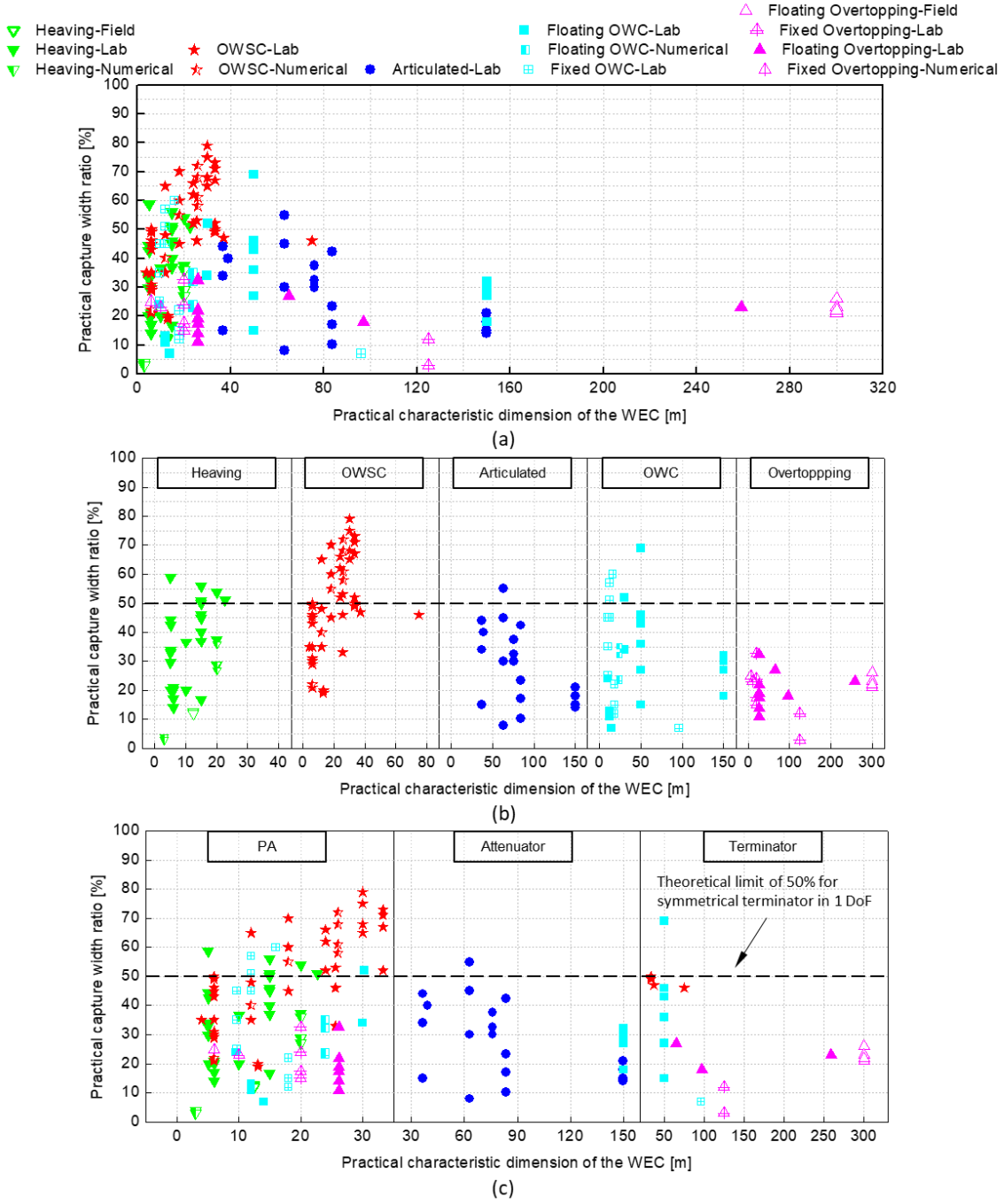

Fig. 8. Practical *CWR*s of WECs as a function of characteristic dimension. (a) Overall view. (b) Subplots classified by working principles. (c) Subplots classified by size & orientation

In addition, as can be seen from Fig. 8(c), PAs have attracted the most interest for study in practice. Of the WECs considered in the dataset, a 63.3% majority is designed as PA in 3D with dimension < 35 m. In theory, due to the antenna effect, PA WECs can unlock the 2D limitations of 50% (for symmetric structures) and 100% (for asymmetric structures) with possibly higher *CWR* > 100%. Although practical efficiency higher than 100% has not been observed by PA, the cases of practical *CWR* greater than 50% indicate that PA is indeed superior to attenuator and terminator WECs in terms of hydrodynamic performance. The relatively high performance efficiency may account for the large research focus on PA presently. Moreover, among the PAs, the OWSC moving in surge appears to perform more efficiently than the PA oscillating in heave (i.e., heaving body and OWC). This fits well with the theoretical finding described in Fig. 7.

For the OWSC, the practical *CW*R appears to have a kind of sensitivity to the device scale. When the scale of OWSC is relatively small (< 30 m), the wider OWSC shows to lead to higher practical *CWR*, reaching up to 80%. This improvement can be attributed to the wider OWSC having a greater proportion of its surface area unaffected by the fluid flowing round the edges than a narrower pitching flap. These practical edge effects reduce as the dimension increases. When the scale of OWSC increases further (> 30 m), the *CWR* reduces as the dimension increases, falling to less than 50%. Findings here for OWSC fit well with the discussions stated by Henry et al., (2010), Renzi and Dias (2012), and Henry et al., (2018). Based on the observations above, it is worth emphasizing again that the common conception of regarding OWSC just as a terminator is unreasonable. As stated in Section 3.1.2, an OWSC with relatively small scale (e.g., 30 m shown in Fig. 8(b)) compared to the wavelength should be regarded as a 'PA' moving in surge, which has the ability of achieving *CWR* higher than 100% and making use of the 'antenna effect' (see Table 1). When the width of an OWSC is comparable with the wavelength and operating as a 'terminator' in 2D, the *CWR* of a symmetrical OWSC can be limited by the theoretical maximum value of 50% (see Table 1).

4.2 Analysis of the practical extracted power

To understand further the real-world performance of the WEC and the gap between practical performance and theoretical limits, the practical extracted power as a function of the WEC dimension is summarized from the database in Appendix A and described in Fig. 9.

Compared with the theoretical scalability for the terminator and attenuator described in Fig. 7, it is not rigorous to conclude the existence of practical scalability through Fig. 9, due to the very small practical sample size for the terminator and attenuator (including OWC, OWSC, articulated body and overtopping).

However, an indicative linear regression line may be drawn for the overtopping type of terminator in Fig. 9, showing that the practical extracted power increases with the device characteristic dimension. For other types of terminator and attenuator, more practical samples are required to draw indicative conclusions.

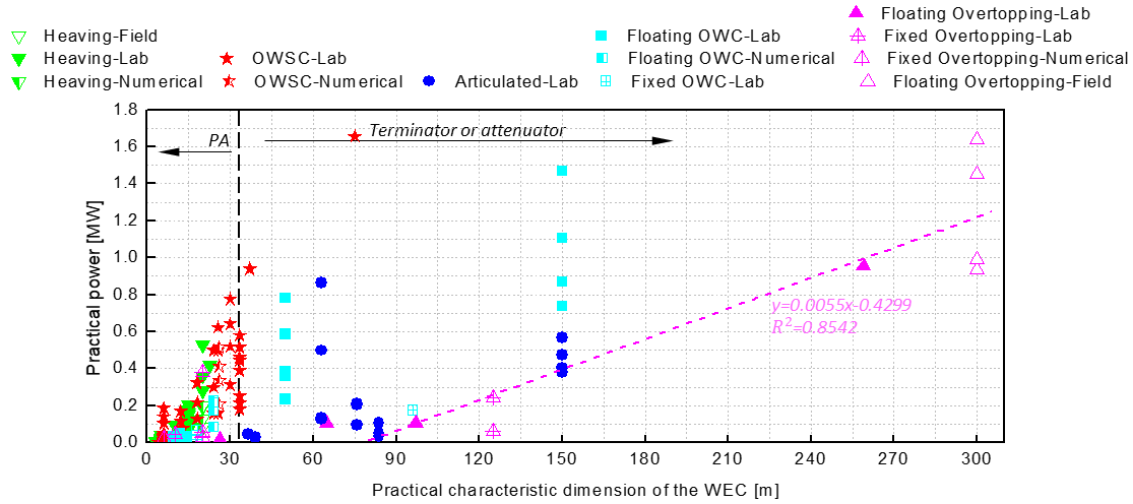

Fig. 9. Practical extracted power of WECs as a function of characteristic dimension. For reference, the dimension size of 35 m is used to clarify the PA and terminator/attenuator. The pink dashed line is the linear regression line for the overtopping device type.

Although it is difficult to clarify the practical scalability, it can be found that the practical capacity of an individual unit has reached MW scale for the WEC acting as terminator (including OWSC, OWC and overtopping) with a relatively large dimension scale ≥ 75 m. For the bulk of the WECs acting as PAs with a small dimension ≤ 35 m, the practical capacities are limited at kW scale. These fit well with the theoretical findings described in Section 3 (see Fig. 7), that without being scalable, the PA's maximum extracted power is limited by the wave resources and is ≤ 1 MW, whereas with the scalability, the terminator can perform at MW scale at the expense of large characteristic dimension.

Due to the relatively large sample size of PA in the database, further practical analysis is conducted here to illustrate the practical power achievable as a function of PA dimension and wave resource and summarized in Fig. 10. It is found that the lack of scalability identified for the PA through the theoretical analysis (see Fig. 7), is consistent in practice as the practical power does not increase proportionally with device dimension. Moreover, it can be seen that, based on the samples included in the database, the maximum practical power for the PA is achieved when the diameter is at 28–31 m and the wave resource is at 35–

45kW/m. This indicates that although without scalability, there exists an optimum diameter for a PA at the selected wave conditions.

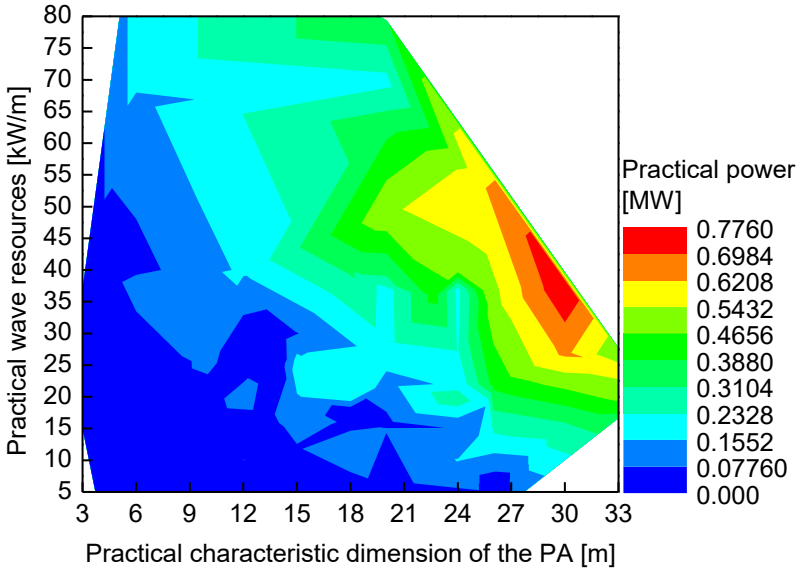

Fig. 10. Practical extracted power of the PA as a function of characteristic dimension and wave resource.

4.3 Recommendations for future WECs

Based on the study described here, we can see that unlike for the wind turbines, the scalability for WECs is much more complex. Therefore, it is unlikely that wave energy will follow the same pathway to development as offshore wind, where the significant scale up of turbines has led to cost reduction. The following recommendations are suggested for future WEC development:

- Despite having limited *CW* and lack of scalability, the hydrodynamic performance efficiency *CWR* is not limited for the PA. The PA WEC has the potential to extract wave energy outside its physical dimension, with *CWR* > 100%. Therefore, rather than chasing MW scale for individual devices that may not be possible for the PA, it is recommended to focus on developing kW scale individual PAs with high efficiency and to achieve MW scale through the deployment of WEC arrays.
- Due to the requirement of a large physical dimension (approximately > 100 m), there exists limited data for terminator and attenuator WECs at demonstration scale. Therefore, more research is needed to understand better the practical scalability of terminator & attenuator devices, and to evaluate whether scaling an individual unit terminator/attenuator to MW level is possible by increasing the device dimension within target costs.

- This work suggests that MW scale units can be achieved by large dimension terminators and attenuators, although little research exists at present. In contrast, much research data exists for PAs but at kW scale. In the short-term, therefore, it is recommended to accelerate the development of the kW scale PAs and their applications into niche markets to achieve commercialisation. A detailed discussion of niche markets for wave energy has been given by Jin and Greaves (2021).
- In the long-term, more studies remain to be done to realise MW scale wave power. The following approaches are recommended in the longer-term pathway towards MW scale wave power: (1) developing single unit terminator or attenuator with increasing dimension to yield MW scale power; (2) developing PA arrays to achieve MW scale; and (3) developing terminator/attenuator arrays.

5. Conclusion

The scalability of WECs is investigated in this work to address the question of whether the performance of a single WEC can be increased by scaling up its size as has been achieved for wind turbines, and whether this approach is an appropriate pathway to the development for wave energy. By reviewing the published resources, fundamental theories and a practical database including 161 WEC cases, the most frequently studied WECs are summarised to demonstrate how scalability works for different WECs in theory and practice. Following main findings and recommendations can be drawn:

- The scalability for WECs is much more complex than for wind turbines. In theory, there exists no scalability for the PA type WEC, but WECs acting as attenuators or terminators are scalable. It is found that (1) regardless of the PA diameter, the theoretical maximum extracted power is constant for a given wave condition and limited by the wave resource and oscillating modes; (2) increasing terminator width can yield a proportional increase in extracted power; (3) increasing attenuator length can generate higher power but not in linear proportion.
- Due to the non-scalability and *CW* limit for PA, it is worth noting that a PA WEC with a diameter approximately < 35 m cannot exceed 1 MW, although MW scales have been achieved for scalable terminator WECs with large width >100 m.
- In both theory and practice, it is found that a PA moving in surge performs better than that in heave motion. In other words, the OWSC type PA performs better than the heaving body.
- Both theory and practice show that the performance of an OWSC is highly sensitive to the device scale. At a small scale, the device acts as a 3D oscillating body in surge motion, *CWR* over 100%

can be achieved and it should be classified as a PA. At a large scale, the device acts as a 2D symmetrical 'terminator' with the maximum *CWR* limited to 50%.

- In theory, PA has the potential to work with high *CWR* and unlock the efficiency limits of 50% and 100% seen for the terminator type WEC. In practice, the PA does show advantage compared with the terminator and attenuator in achieving high performance efficiency (*CWR*). Some PAs have demonstrated practical efficiencies > 50%, but most of the practical efficiencies for terminator and attenuator are less than 50%.
- In the short-term, instead of developing MW scale WECs to compete with the offshore wind at grid scale, it is recommended first to facilitate the development of the kW scale PA unit and the corresponding niche applications to realise commercialisation. In the long-term, more research remains to be done to understand the benefits of using their inherent scalability to yield MW scale terminator or attenuator WECs and in comparison, the alternative of using PA arrays to realise MW scale. Rather than a single converged design for wave energy, converged designs for different categories of WEC may emerge; the three main WEC categories (as summarised in Table 1) considered in this work show different characteristics and scalabilities and are likely to follow different pathways to development and to reach commercialisation.

It worth noting that a WEC with scalability, a high *CWR* and the operation in the energetic site is not necessary a WEC with the lowest cost. It could be that a WEC producing electricity at the lowest LCoE has no scalability, a low *CWR* and the deployment at the moderate resource, but has a long-life expectancy, easy accessibility, and low cost for operation & maintenance. Further work, studying the joint effects of the WEC scalability, site selection, accessibility, reliability and survivability, and operation and maintenance on the LCoE is thus required in the future to understand better the potential of cost reduction for the wave energy sector.

Appendix A. The database summarising the practical performances of different WECs

It should be noted that considering the oscillating modes of operation, some WECs operate in multi-modes. For simplification, the WECs listed in the database are classified based on the dominant oscillating mode. For example, a single Wavestar model has the motions in heave, surge, and pitch, but is heave-dominated (Windt, Davidson et al. 2021). This device is, therefore, classified as the heaving body in the database.

Working principle	Device	Orientation & size	Characteristic dimension (m)	CWR (%)	Wave Resource (kW/m)	Method	PTO	Ref.
Heaving body	Danish Wave Power	Point absorber	10/diameter	20	16	Lab test	Mechanical damping	(Babarit , 2015)
	Wavebob	Point absorber	15/diameter	40	12	N/A	N/A	(Babarit , 2015)
				51	21			
				46	26			
				45	15			
	AquaBuOY	Point absorber	6/diameter	20	12	N/A	N/A	(Babarit , 2015)
				17	21			
				14	26			
				21	15			
	LifeSaver	Point absorber	12.5/diameter	12.5	27	Field test	Permanent magnet synchronous generator	(Sjolte et al., 2013)
				12	26			
	Bottom-referenced buoy	Point absorber	3/diameter	4	15	Numerical modeling	Numerical Damping	(Babarit et al., 2012)
				4	22			
				4	27			
				3	37			
	Self-reacting point absorbers	Point absorber	15/diameter	50	16	Lab test	Linear actuator	(Beatty et al., 2015)
				50	20			
				56	24			
				37	27			
				16.7	30			
	1:20 scale single Wavestar model	Point absorber	5.08/diameter	42.5	8.8	Lab test	linear actuator	(Zurkinden et al., 2014)
				20	15.3			
	RM3	Point absorber	20/diameter	28.7	62.78	Lab test	Hydraulic piston	(Yu et al., 2015)
				53.9	48.97			
				37.4	37.8			
			10/diameter	36.7	25.5			
	Small bottom-referenced heaving buoy	Point absorber	3/diameter	4	15	Numerical modeling	Numerical Damping	(Babarit et al., 2012)
				4	22			
				4	27			
				3	37			
	Floating two-body heaving converter	Point absorber	20/diameter	27	15	Numerical modeling	Numerical Damping	(Babarit et al., 2012)
				29	22			
				36	27			
				27	37			
	Two-body WEC	Point absorber	22.69	51.06	36	Lab test	Linear generator	(Martin et al., 2020)
	Direct-drive WEC	Point absorber	5/diameter	33.87	5.34	Lab test	Linear generator	(Zhang et al., 2018)
				32.87	7.68			
				29.75	9.49			
				44.41	10.75			
				58.77	12.65			
OWSC	Wave-driven, resonant, arcuate action, Surging-Point-Absorber	Point absorber	25.6/width	33	18.6	Lab test	Mechanical damping	(Rahmati and Aggidis, 2016)
				53	36.8			
				46	52.8			
	BioPower	Point absorber	6/width	50	5.4	Lab test	Viscous dashpot	(Flocard and Finnigan, 2010; Babarit, 2015)
				49	8.45			
				49	10.37			
				29	28			
				35	66			
				43	71.4			
				31	99.2			
				45	38.5			
	Oyster example	Point absorber	6/width	46	10	Lab test	Disk-brake and calliper system	(Henry et al., 2010; Henry et al., 2018)
			12/width	65	10			
			18/width	70	10			
			24/width	66	10			
			6/width	30	20			
			12/width	48	20			
			18/width	60	20			
			24/width	62	20			
			6/width	21	40			
			12/width	35	40			
			18/width	45	40			
			24/width	52	40			

	Moular OWSC	Terminator	33.3/width	49	11	Lab test	Magnetic particle brake	(Wilkinson et al., 2017)
				49	13			
				50	15			
				67	17.34			
				73	18.25			
				73	21.1			
				71	24.5			
				52	26.5			
	OWSC	Point absorber	6/width	22	N/A	Numerical modelling	Numerical damping	(Renzi and Dias, 2012)
			12/width	40	N/A			
			18/width	55	N/A			
	Ediburgh Duck	Terminator	37/width	47	54	Lab test	N/A	(Babarit, 2015)
		Point absorber	30/width	65	16			
				79	27			
				68	38			
				75	23			
	Bristol Cylinder	Terminator	75/width	46	48	Lab test	N/A	(Babarit, 2015)
	OWSC	Point absorber	13.1/width	20	28.46	Lab test	Hydraulic cylinder	(Brito et al., 2020)
				19	15.8			
	OWSC	Point absorber	4/width	35	1.12	Lab test	Magnetic powder brake	(Ning et al., 2017)
	Bottom fixed OWSC	Point absorber	26/width	61	13	Numerical modelling	N/A	(Babarit et al., 2012)
				68	19			
				72	22			
				58	34			
Articulated body	Pelamis	Attenuator	150/length	21	12	Lab test	N/A	(Babarit, 2015)
				15	21			
				14	27			
				18	15			
	DEXA	Attenuator	63/length	55	14.37	Lab test	Pneumatic dashpot	(Zanuttigh et al., 2013)
				45	30.5			
				8	26			
				30	6.5			
	Inspired McCabe Wave Pump	Attenuator	39.2/length	40	1.79	Lab test	Mechanical damping	(Paparella and Ringwood, 2016)
	M100 of the Mocean Energy	Attenuator	36.7/length	34	3.76	Lab test	Motor	(McNatt and Retzler, 2020)
				15	8.19			
				44	2.48			
	M4-3 floaters	Attenuator	76/length	30	9.1	Lab test	Pneumatic dashpot	(Stansby et al., 2015)
				32.5	3.762			
				37.5	3.39			
				32.5	8.2			
	SeaPower Platform	Attenuator	83.75/length	42.4	2.9	Lab test	Motor	(Cian and Atlantic, 2014)
				23.4	2.44			
				17.1	3.36			
				10.24	3.78			
OWC-floating	Floating OWC with TLP	Point absorber	9.54/width	24	13.75	Lab test	Air orifice	[25]
	Coaxial-duct OWC	Point absorber	14/diameter	7	30.5	Lab test	Air orifice	(Singh et al., 2020)
				7	25			
	Spar buoy	Point absorber	12/diameter	13	30.5	Lab test	Air orifice	(Portillo et al., 2020)
				11	25			
	Novel dual chamber OWC	Terminator	50/width	43	16.97		Air orifice	(Xu et al., 2020)
				36	19.8			
				69	22.63			
				46	25.46			
				27	28.28			
				15	31.11			
	Backward bednt duct buoy (BBDB)	Point absorber	24\width	23	15	Numerical modelling	N/A	(Babarit, 2015)
				32	22			
				35	27			
				24	37			
	KNSWING	Attenuator	150/length	30	16.34	Lab test	Air orifice	(Kim and
				32	18.14			

				27	27.25			Kim, 2015)
				18	54.36			
	BBDB	Point absorber	30.3/width	52	N/A	Lab test	N/A	(Wu et al., 2018)
	Mighty Whale	Point absorber	30/width	34	N/A	Lab test	N/A	(Wu et al., 2018)
OWC-fixed	Mutriku wave power plant	Terminator	96/width	7	26	Lab test	N/A	(Babarit , 2015)
	Fixed cylinderical dual chamber OWC	Point absorber	12/diameter	51	1.82	Lab test	Air orifice	(Ning et al., 2020)
				57	2.38			
				45	2.65			
				11	3.77			
	Fixed L shape OWC	Point absorber	9.72/width	35	4.95	Lab test	Air orifice	(Rezanejad et al., 2019)
				45	4.33			
				25	5.57			
	Fixed OWC	Point absorber	18/width	22	16	Lab test	Air orifice	(Tseng et al., 2000)
				12	18			
				15	5.76			
	Fixed dual-chmber OWC	Point absorber	16/width	60	1.85	Lab test	Air orifice	(Ning et al., 2019)
Overtopping -floating	Wavedragon	Terminator	300/width	26	12	Field test	Propeller turbines	(Babarit , 2015)
				23	21			
				21	26			
				22	15			
			65/width	27	6	Lab test	N/A	
			97/width	18	6			
			259/width	23	16			
	Conical structure	Point abosrber	26.13/diameter	14	2.98	Lab test	Discharges	(Tanaka et al., 2009)
				19	2.61			
				22	2.23			
				32.5	1.49			
				17.5	3.81			
				11	5.96			
Overtopping -fixed	SSG	Point absorber	10/width	23	19.5	Lab test	Discharges	(Babarit , 2015)
	Power Pyramid	Terminator	125/width	12	16	Lab test	Discharges	(Babarit , 2015)
	Sucking Sea Shaft	Terminator		3	16	Lab test	Discharges	(Babarit , 2015)
	Overtopping-OWC hybrid	Point absorber	20/width	32.7	4.11	Lab test	N/A	(Calheiros-Cabral et al., 2020)
				17.5	15.64			
				24	79.4			
				15	69.8			
	OBREC	Point absorber	6/width	25	12.86	Numerical modelling	N/A	(Contestabile and Vicinanza, 2018)

Acknowledgments

This work was conducted within the Supergen Offshore Renewable Energy (ORE) Hub, a £9 Million programme 2018–2023 funded by Engineering and Physical Sciences Research Council (EPSRC) under No. EP/S000747/1.

References

Aderinto, T. and H. Li (2018). "Ocean wave energy converters: Status and challenges." Energies **11**(5): 1250, https://doi.org/1210.3390/en11051250.

Aderinto, T. and H. Li (2019). "Review on power performance and efficiency of wave energy converters." Energies **12**(22): 4329, https://doi.org/4310.3390/en12224329.

Antonio, F. d. O. (2010). "Wave energy utilization: A review of the technologies." Renew Sustain Energy Rev **14**(3): 899-918, https://doi.org/810.1016/j.rser.2009.1011.1003.

AQUARET. (2012). from http://www.aquaret.com. [Accessed on 01/04/2021].

AWS. from https://www.awsocean.com/research-development. [Accessed on 14/07/2021].

Babarit, A. (2015). "A database of capture width ratio of wave energy converters." Renew Energy **80**: 610-628, https://doi.org/610.1016/j.renene.2015.1002.1049.

Babarit, A. (2017). Ocean wave energy conversion: resource, technologies and performance, Elsevier.

Babarit, A., J. Hals, M. J. Muliawan, A. Kurniawan, T. Moan and J. Krokstad (2012). "Numerical benchmarking study of a selection of wave energy converters." Renew energy **41**: 44-63, https://doi.org/10.1016/j.renene.2011.1010.1002.

Beatty, S. J., M. Hall, B. J. Buckham, P. Wild and B. Bocking (2015). "Experimental and numerical comparisons of self-reacting point absorber wave energy converters in regular waves." Ocean Eng **104**: 370-386, https://doi.org/310.1016/j.oceaneng.2015.1005.1027.

Bedard, R. and G. Hagerman. (2004). "E2I EPRI assessment offshore wave energy conversion devices." Electrical Innovation Institute: Washington, DC, USA, from https://en.calameo.com/books/0006774702078bff76594. [Accessed on 15/04/2021].

Betz, A. (1920). "Das Maximum der theoretisch möglichen Ausnutzung des Windes durch Windmotoren." Zeitschrift fur das gesamte Turbinenwesten **20**.

BEIS (2019). Budget Notice for CFD Allocation Round 3.

BEIS. (2020). "Contracts for difference for low carbon electricity generation - consultation on proposed amendments to the scheme." from https://assets.publishing.service.gov.uk/government/uploads/system/uploads/attachment_data/file/885248/cfd-ar4-proposed-amendments-consultation.pdf. [Accessed on 25/06/2021].

Beyene, A. and J. H. Wilson (2006). "Comparison of wave energy flux for northern, central, and southern coast of California based on long-term statistical wave data." Energy **31**(12): 1856-1869, https://doi.org/1810.1016/j.energy.2005.1808.1008.

BioWave. (2015). "BioWave Port Fairy Pilot Wave Energy Project." from https://tethys.pnnl.gov/project-sites/biowave-port-fairy-pilot-wave-energy-project. [Accessed on 27/07/2021].

Boake, C. B., T. J. Whittaker, M. Folley and H. Ellen. (2002). "Overview and initial operational experience of the LIMPET wave energy plant." The Twelfth International Offshore and Polar Engineering Conference, from https://citeseerx.ist.psu.edu/viewdoc/download?doi=10.1.1.473.2780&rep=rep1&type=pdf. [Accessed on 18/07/2021].

Brito, M., R. M. Ferreira, L. Teixeira, M. G. Neves and R. B. Canelas (2020). "Experimental investigation on the power capture of an oscillating wave surge converter in unidirectional waves." Renew Energy **151**: 975-992, https://doi.org/910.1016/j.renene.2019.1011.1094.

Budal, K. and J. Falnes (1975). "A resonant point absorber of ocean-wave power." Nature **256**(5517): 478-479, https://doi.org/410.1038/257626c257620.

Caduff, M., M. A. Huijbregts, H.-J. Althaus, A. Koehler and S. Hellweg (2012). "Wind power electricity: the bigger the turbine, the greener the electricity?" Envir Sci Tech **46**(9): 4725-4733, https://doi.org/4710.1021/es204108n.

Calheiros-Cabral, T., D. Clemente, P. Rosa-Santos, F. Taveira-Pinto, V. Ramos, T. Morais and H. Cestaro (2020). "Evaluation of the annual electricity production of a hybrid breakwater-integrated wave energy converter." Energy: 118845, https://doi.org/118810.111016/j.energy.112020.118845.

Carnegie. (2021). from https://www.carnegiece.com/ceto-technology. [Accessed on 27/07/2021].

CCell-Wave. (2021). from https://www.ccell.co.uk/technology. [Accessed on 18/07/2021].

Cian, M. and S. Atlantic. (2014). "SeaPower Platform Configuration Test Program." from https://www.marinet2.eu/wp-content/uploads/2017/04/SPPCTP_QUB_Infrastructure_Access_Report.pdf. [Accessed on 18/07/2021].

Coe, R. G. and V. S. Neary. (2014). "Review of methods for modeling wave energy converter survival in extreme sea states." from https://vtechworks.lib.vt.edu/handle/10919/49221. [Accessed on 06/02/2021].

Coe, R. G., Y.-H. Yu and J. Van Rij (2018). "A survey of wec reliability, survival and design practices." Energies **11**(1): 4, https://doi.org/10.3390/en11010004.

Collinsa, I., M. Hossaina, W. Dettmera and I. Mastersa. (2021). "Flexible membrane structures for wave energy harvesting: A review of the developments, materials and computational modelling approaches." from https://www.researchgate.net/profile/Mokarram-Hossain-2/publication/353018206_Flexible_membrane_structures_for_wave_energy_harvesting_A_review_of_the_developments_materials_and_computational_modelling_approaches/links/60e46c99a6fdccb7450cc8c7

/Flexible-membrane-structures-for-wave-energy-harvesting-A-review-of-the-developments-materials-and-computational-modelling-approaches.pdf. [Accessed on 18/07/2021].

Contestabile, P. and D. Vicinanza (2018). "Coastal defence integrating wave-energy-based desalination: a case study in Madagascar." J Mar Sci and Eng **6**(2): 64, https://doi.org/10.3390/jmse6020064.

Cornejo-Bueno, L., J. Nieto-Borge, P. García-Díaz, G. Rodríguez and S. Salcedo-Sanz (2016). "Significant wave height and energy flux prediction for marine energy applications: A grouping genetic algorithm–Extreme Learning Machine approach." Renew Energy **97**: 380-389, https://doi.org/310.1016/j.renene.2016.1005.1094.

CORPOWER. (2021). from https://www.corpowerocean.com. [Accessed on 01/04/2021].

Cotten, A. and D. Forehand (2020). "Maximum wave-power absorption under motion constraints associated with both controlled and uncontrolled degrees of freedom." Appl Ocean Res **100**: 102194, https://doi.org/102110.101016/j.apor.102020.102194.

ECORYS and Fraunhofer. (2017). "Study on Lessons for Ocean Energy Development." from http://publications.europa.eu/resource/cellar/03c9b48d-66af-11e7-b2f2-01aa75ed71a1.0001.01/DOC_1. [Accessed on 10/05/2021].

Evans, D. (1976). "A theory for wave-power absorption by oscillating bodies." J Fluid Mech **77**(1): 1-25, https://doi.org/10.1017/S0022112076001109.

Evans, D. (1978). "The oscillating water column wave-energy device." IMA Journal of Applied Mathematics **22**(4): 423-433, https://doi.org/410.1093/imamat/1022.1094.1423.

Evans, D. (1981). "Maximum wave-power absorption under motion constraints." Appl Ocean Res **3**(4): 200-203, https://doi.org/210.1016/0141-1187(1081)90063-90068.

Evans, D. and R. Porter (1995). "Hydrodynamic characteristics of an oscillating water column device." Appl Ocean Res **17**(3): 155-164, https://doi.org/110.1016/0141-1187(1095)00008-00009.

Evans, D. V. and R. Porter (1997). "Efficient calculation of hydrodynamic properties of OWC-type devices." J Offshore Mech Arct Eng **119**(4): 210-218, https://doi.org/210.1115/1111.2829098.

Even, H. (2019). "Introduction to bolt sea power wave energy conversion techonology by fred. olsen." from https://energyvalley.no/wp-content/uploads/2019/04/Powering-offshore-systems-on-ocean-waves-%E2%80%93-technology-deployments-and-applications-Fred-Olsen-BOLT-Sea-Power.pdf. [Accessed on 03/04/2021].

Falnes, J. (2007). "A review of wave-energy extraction." Mar Struct **20**(4): 185-201, https://doi.org/110.1016/j.marstruc.2007.1009.1001.

Falnes, J. and A. Kurniawan (2020). Ocean waves and oscillating systems: linear interactions including wave-energy extraction, Cambridge university press.

Falnes, J. and P. McIver (1985). "Surface wave interactions with systems of oscillating bodies and pressure distributions." Appl Ocean Res **7**(4): 225-234, https://doi.org/210.1016/0141-1187(1085)90029-X.

Farley, F. (1982). "Wave energy conversion by flexible resonant rafts." Appl Ocean Res **4**(1): 57-63, https://doi.org/10.1016/S0141-1187(1082)80022-80029.

Flocard, F. and T. Finnigan (2010). "Laboratory experiments on the power capture of pitching vertical cylinders in waves." Ocean Eng **37**(11-12): 989-997, https://doi.org/910.1016/j.oceaneng.2010.1003.1011.

Ghisu, G. and P. Carabotta. (2017). "Ocean Energy exploitation in Italy: ongoing R&D activities." from https://www.enea.it/en/publications/abstract/ocean-energy-italy. [Accessed on 15/07/2021].

Gomes, R., L. Gato, A. Falcao, J. Henriques, P. Vicente, P. Ruiz-Minguela, J. V. Varandas and L. Trigo. (2013). "Experimental Validation of a Spar Buoy Design for Wave Energy Conversion." Marinet, Lisboa, from https://www.marinet2.eu/wp-content/uploads/2017/04/SPAR-BUOY-WEC_NAREC_Infrastructure_Access_Report-1.pdf. [Accessed on 18/07/2021].

Greaves, D. and G. Iglesias (2018). Wave and tidal energy, John Wiley & Sons.

Greaves, D. and S. Jin. (2020). "Wave energy road map." from https://epsrc.ukri.org/files/funding/calls/2020/wave-energy-road-map. [Accessed on 12/07/2021].

Greaves, D., S. Jin, H. Jeffrey, C. Cochrane, S. Pennock and L. Richards. (2020). "Wave Energy Innovation Position Paper." from https://supergen-ore.net/uploads/resources/Wave_Energy_Innovation_-_Position_Paper.pdf. [Accessed on 10/07/2021].

Hannon, M., R. van Diemen and J. Skea. (2017). "Examining the Effectiveness of Support for UK Wave Energy Innovation since 2000: Lost at Sea or a New Wave of Innovation?", from https://strathprints.strath.ac.uk/62210/. [Accessed on 18/07/2021].

Haren, P. (1979). "Optimal design of Hagen-Cockerall raft." from https://dspace.mit.edu/bitstream/handle/1721.1/57715/07517390-MIT.pdf?sequence=2. [Accessed on 18/07/2021].

He, F., H. Zhang, J. Zhao, S. Zheng and G. Iglesias (2019). "Hydrodynamic performance of a pile-supported OWC breakwater: an analytical study." Appl Ocean Res **88**: 326-340, https://doi.org/310.1016/j.apor.2019.1003.1022.

Henry, A., K. Doherty, L. Cameron, T. Whittaker and R. Doherty (2010). "Advances in the design of the Oyster wave energy converter." RINA Marine and Offshore Renewable Energy, London, UK.

Henry, A., M. Folley and T. Whittaker (2018). "A conceptual model of the hydrodynamics of an oscillating wave surge converter." Renew Energy **118**: 965-972, https://doi.org/910.1016/j.renene.2017.1010.1090.

IRENA. (2019). "Future of wind-Deployment, investment, technology, grid integration and socio-economic aspects." from https://www.irena.org/-/media/Files/IRENA/Agency/Publication/2019/Oct/IRENA_Future_of_wind_2019.pdf. [Accessed on 18/072021].

Iuppa, C., L. Cavallaro, R. E. Musumeci, D. Vicinanza and E. Foti (2019). "Empirical overtopping volume statistics at an OBREC." Coast Eng **152**: 103524, https://doi.org/103510.101016/j.coastaleng.102019.103524.

Jin, S. and D. Greaves (2021). "Wave energy in the UK: Status review and future perspectives." Renew Sustain Energy Rev **143**: 110932, https://doi.org/110910.111016/j.rser.112021.110932.

Journée, J. M. J. and W. W. Massie. (2001). "Offshore hydrodynamics." from https://ocw.tudelft.nl/wp-content/uploads/OffshoreHydromechanics_Journee_Massie.pdf. [Accessed on 29/07/2021].

Kim, N. and N. Kim. (2015). "KNSWING Attenuator development phase I." from https://www.marinet2.eu/wp-content/uploads/2017/04/MARINET-KNSWING-1b-Portaferry_-mooring_Final.pdf. [Accessed on 15/06/2021].

Kraemer, D. R., M. McCormick and C. O. Ohl (2001). "Comparison of experimental and theoretical results of the motions of a McCabe Wave Pump."

Lavidas, G. (2020). "Selection index for Wave Energy Deployments (SIWED): A near-deterministic index for wave energy converters." Energy **196**: 117131, https://doi.org/117110.111016/j.energy.112020.117131.

Lavidas, G. and K. Blok (2021). "Shifting wave energy perceptions: The case for wave energy converter (WEC) feasibility at milder resources." Renew Energy **170**: 1143-1155, https://doi.org/1110.1016/j.renene.2021.1102.1041.

Marine, R. (2021). from https://www.resolutemarine.com/technology. [Accessed on 18/07/2021].

MARMOK-A-5. (2016). from https://tethys.pnnl.gov/project-sites/marmok-5-wave-energy-converter. [Accessed on 18/07/2021].

Martin, D., X. Li, C.-A. Chen, K. Thiagarajan, K. Ngo, R. Parker and L. Zuo (2020). "Numerical analysis and wave tank validation on the optimal design of a two-body wave energy converter." Renew Energy **145**: 632-641, https://doi.org/610.1016/j.renene.2019.1005.1109.

Martins-Rivas, H. and C. C. Mei (2009). "Wave power extraction from an oscillating water column at the tip of a breakwater." J Fluid Mech **626**: 395-414, https://doi.org/310.1017/S0022112009005990.

Mavrakos, S. A. and D. N. Konispoliatis (2012). "Hydrodynamics of a free floating vertical axisymmetric oscillating water column device." J Appl Math **2012**: https://doi.org/10.1155/2012/142850.

McNatt, J. C. and C. H. Retzler (2020). "The performance of the Mocean M100 wave energy converter described through numerical and physical modelling." International Marine Energy Journal **3**(1): 11-19, https://doi.org/10.36688/imej.36683.36611-36619.

Mehlum, E. (1986). Tapchan. Hydrodynamics of Ocean Wave-Energy Utilization, Springer**:** 51-55.

Mei, C. C. (1976). "Power extraction from water waves." JShR **20**: 63-66.

MeyGen. (2021). from https://simecatlantis.com/projects/meygen. [Accessed on 10/06/2021].

Mocean. (2021). from https://www.mocean.energy/wave-energy-converter. [18/07/2021].

Newman, J. (1976). The interaction of stationary vessels with regular waves. Proceedings of the 11th Symposium on Naval Hydrodynamics, London, 1976.

Newman, J. (1979). "Absorption of wave energy by elongated bodies." Appl Ocean Res **1**(4): 189-196, https://doi.org/110.1016/0141-1187(1079)90026-90029.

Nielsen, K. and J. B. Thomsen (2019). "KNSwing—On the Mooring Loads of a Ship-Like Wave Energy Converter." J Mar Sci Eng **7**(2): 29, https://doi.org/10.3390/jmse7020029.

Ning, D.-z., R.-q. Wang, L.-f. Chen and K. Sun (2019). "Experimental investigation of a land-based dual-chamber OWC wave energy converter." Renew Sustain Energy Rev **105**: 48-60, https://doi.org/10.1016/j.rser.2019.1001.1043.

Ning, D.-z., Y. Zhou, R. Mayon and L. Johanning (2020). "Experimental investigation on the hydrodynamic performance of a cylindrical dual-chamber Oscillating Water Column device." Appl Energy **260**: 114252, https://doi.org/114210.111016/j.apenergy.112019.114252.

Ning, D., C. Liu, C. Zhang, M. Goteman, H. Zhao and B. Teng (2017). "Hydrodynamic performance of an oscillating wave surge converter in regular and irregular waves: an experimental study." J Mar Sci and Technol **25**(5): 520-530, https://jmstt.ntou.edu.tw/journal/vol525/iss525/524.

OceanEnergy. (2020). from https://oceanenergy.ie/oe-buoy. [Accessed on 18/07/2021].

OES. (2010–2020). "Ocean energy systems annual reports." from https://www.ocean-energy-systems.org/publications/oes-annual-reports. [Accessed on 24/06/2021].

OPT. (2021). from https://oceanpowertechnologies.com/pb3-powerbuoy. [Accessed on 21/07/2021].

Osawa, H., Y. Washio, T. Ogata, Y. Tsuritani and Y. Nagata (2002). The Offshore Floating Type Wave Power Device" Mighty Whale" Open Sea TestsPerformance of The Prototype–. The Twelfth International Offshore and Polar Engineering Conference, International Society of Offshore and Polar Engineers.

Paparella, F. and J. V. Ringwood (2016). Enhancement of the wave energy conversion characteristics of a hinge-barge using pseudospectral control. 2016 UKACC 11th International Conference on Control (CONTROL), IEEE.

Pelamis. (2004). from http://www.emec.org.uk/about-us/wave-clients/pelamis-wave-power. [Accessed on 18/07/2021].

Pizer, D. (1993). "Maximum wave-power absorption of point absorbers under motion constraints." Appl Ocean Res **15**(4): 227-234, https://doi.org/210.1016/0141-1187(1093)90011-L.

Porter, R., S. Zheng and D. Greaves (2021). "Extending limits on wave power absorption by axisymmetric devices." J Fluid Mech. https://doi.org/10.1017/jfm.2021.645.

Portillo, J., K. Collins, R. Gomes, J. Henriques, L. Gato, B. Howey, M. Hann, D. Greaves and A. Falcão (2020). "Wave energy converter physical model design and testing: The case of floating oscillating-water-columns." Appl Energy **278**: 115638, https://doi.org/115610.111016/j.apenergy.112020.115638.

Rahmati, M. and G. A. Aggidis (2016). "Numerical and experimental analysis of the power output of a point absorber wave energy converter in irregular waves." Ocean Eng **111**: 483-492, https://doi.org/410.1016/j.oceaneng.2015.1011.1011.

Rainey, R. (2001). The Pelamis wave energy converter: it may be jolly good in practice, but will it work in theory. Proc. 16th Int'l. Workshop on Water Waves and Floating Bodies.

Rendel, P. and C. E. Tritton. (1982). "Consultants' 1981 Assessment: Preliminary Information." from http://www.homepages.ed.ac.uk/shs/MIT%20visit/9_Official%20Consultant%20Assessment%201981.pdf. [Accessed on 17/07/2021].

Renzi, E. and F. Dias (2012). "Resonant behaviour of an oscillating wave energy converter in a channel." J Fluid Mech **701**: 482-510, https://doi.org/410.1017/jfm.2012.1194.

Rezanejad, K., A. Souto-Iglesias and C. G. Soares (2019). "Experimental investigation on the hydrodynamic performance of an L-shaped duct oscillating water column wave energy converter." Ocean Eng **173**: 388-398, https://doi.org/310.1016/j.oceaneng.2019.1001.1009.

Santo, H., P. Taylor and P. Stansby (2020). "The performance of the three-float M4 wave energy converter off Albany, on the south coast of western Australia, compared to Orkney (EMEC) in the UK." Renew Energy **146**: 444-459, https://doi.org/410.1016/j.renene.2019.1006.1146.

Santo, H., P. H. Taylor, E. C. Moreno, P. Stansby, R. E. Taylor, L. Sun and J. Zang (2017). "Extreme motion and response statistics for survival of the three-float wave energy converter M4 in intermediate water depth." J Fluid Mech **813**: 175-204, https://doi.org/110.1017/jfm.2016.1872.

SEABASED. (2021). from https://seabased.com. [Accessed on 29/07/2021].

SEAPOWER. (2021). from http://www.seapower.ie/our-technology. [Accessed on 18/07/2021].

Sheng, W. (2019). "Wave energy conversion and hydrodynamics modelling technologies: A review." Renew Sustain Energy Rev **109**: 482-498, https://doi.org/410.1016/j.rser.2019.1004.1030.

Singh, U., N. Abdussamie and J. Hore (2020). "Hydrodynamic performance of a floating offshore OWC wave energy converter: An experimental study." Renew Sustain Energy Rev **117**: 109501, https://doi.org/109510.101016/j.rser.102019.109501.

Sjolte, J., I. Bjerke, G. Tjensvoll and M. Molinas (2013). Summary of performance after one year of operation with the lifesaver wave energy converter system. EWTEC13.

Smart, G. and M. Noonan. (2018). "Tidal stream and wave energy cost reduction and industrial benefit." from https://www.marineenergywales.co.uk/wp-content/uploads/2018/05/ORE-Catapult-Tidal-Stream-and-Wave-Energy-Cost-Reduction-and-Ind-Benefit-FINAL-v03.02.pdf. [Accesses on 18/07/2021].

Stansby, P., E. C. Moreno and T. Stallard (2015). "Capture width of the three-float multi-mode multi-resonance broadband wave energy line absorber M4 from laboratory studies with irregular waves of different spectral shape and directional spread." J Ocean Eng Mar Energy **1**(3): 287-298, https://doi.org/210.1007/s40722-40015-40022-40726.

Stansby, P., E. C. Moreno and T. Stallard (2017). "Large capacity multi-float configurations for the wave energy converter M4 using a time-domain linear diffraction model." Appl Ocean Res **68**: 53-64, https://doi.org/10.1016/j.apor.2017.1007.1018.

Stansell, P. and D. J. Pizer (2013). "Maximum wave-power absorption by attenuating line absorbers under volume constraints." Appl Ocean Res **40**: 83-93, https://doi.org/10.1016/j.apor.2012.1011.1005.

Tanaka, H., A. Sumita, A. Suzuki and Y. Manabe (2009). Experimental Study on Water Flow Characteristics of Conical Floating Structure. International Conference on Offshore Mechanics and Arctic Engineering.

Torre-Enciso, Y., I. Ortubia, L. L. De Aguileta and J. Marqués (2009). Mutriku wave power plant: from the thinking out to the reality. 8th EWTEC, https://tethys.pnnl.gov/sites/default/files/publications/Torre-Enciso_et_al_2009.pdf. [Accessed on 29/07/2021].

Tseng, R.-S., R.-H. Wu and C.-C. Huang (2000). "Model study of a shoreline wave-power system." Ocean Eng **27**(8): 801-821, https://doi.org/810.1016/S0029-8018(1099)00028-00021.

UK-Parliament. (2001). "Science and techonology seventh report: wave and tidal energy." from https://publications.parliament.uk/pa/cm200001/cmselect/cmsctech/291/29104.htm. [Accessed on 26/06/2021].

WaveDragon. (2017). from http://www.wavedragon.co.uk/technology-2. [Accessed on 29/07/2021].

WaveRoller. (2021). from https://aw-energy.com/waveroller. [Accessed on 01/04/2021].

Wilkinson, L., T. Whittaker, P. Thies, S. Day and D. Ingram (2017). "The power-capture of a nearshore, modular, flap-type wave energy converter in regular waves." Ocean Eng **137**: 394-403, https://doi.org/310.1016/j.oceaneng.2017.1004.1016.

Windt, C., et al. (2021). "Numerical analysis of the hydrodynamic scaling effects for the Wavestar wave energy converter." J Fluids Struct **105**: 103328, https://doi.org/103310.101016/j.jfluidstructs.102021.103328.

Wu, B., T. Chen, J. Jiang, G. Li, Y. Zhang and Y. Ye (2018). "Economic assessment of wave power boat based on the performance of “Mighty Whale” and BBDB." Renew Sustain Energy Rev **81**: 946-953, https://doi.org/910.1016/j.rser.2017.1008.1051.

Wu, J., Y. Yao, L. Zhou, N. Chen, H. Yu, W. Li and M. Göteman (2017). "Performance analysis of solo Duck wave energy converter arrays under motion constraints." Energy **139**: 155-169, https://doi.org/110.1016/j.energy.2017.1007.1152.

Xu, S., K. Rezanejad, J. Gadelho, S. Wang and C. G. Soares (2020). "Experimental investigation on a dual chamber floating oscillating water column moored by flexible mooring systems." Ocean Eng **216**: 108083, https://doi.org/108010.101016/j.oceaneng.102020.108083.

Yde, A., T. J. Larsen, A. M. Hansen, M. Fernandez, S. Bellew and F. P. Plant (2015). Comparison of simulations and offshore measurement data of a combined floating wind and wave energy demonstration platform. J Ocean Wind Energy, ISOPE. **2:** 129-137, http://publications.isope.org/jowe/jowe-102-123/jowe-102-123-p129-jcr134-Yde.pdf. [Accessed on 118/107/2021].

Yu, Y., M. Lawson, Y. Li, M. Previsic, J. Epler and J. Lou (2015). Experimental wave tank test for reference model 3 floating-point absorber wave energy converter project, NREL, https://www.nrel.gov/docs/fy15osti/62951.pdf. [Accessed on 27/07/2021].

Zanuttigh, B., E. Angelelli and J. P. Kofoed (2013). "Effects of mooring systems on the performance of a wave activated body energy converter." Renew Energy **57**: 422-431, https://doi.org/410.1016/j.renene.2013.1002.1006.

Zhang, J., H. Yu and Z. Shi (2018). "Design and Experiment Analysis of a Direct-Drive Wave Energy Converter with a Linear Generator." Energies **11**(4): 735, https://doi.org/710.3390/en11040735.

Zheng, S., Y. Zhang and G. Iglesias (2019). "Coast/breakwater-integrated OWC: A theoretical model." Mar Struct **66**: 121-135, https://doi.org/110.1016/j.marstruc.2019.1004.1001.

Zurkinden, A. S., F. Ferri, S. Beatty, J. P. Kofoed and M. Kramer (2014). "Non-linear numerical modeling and experimental testing of a point absorber wave energy converter." Ocean Eng **78**: 11-21, https://doi.org/10.1016/j.oceaneng.2013.1012.1009.